e-J. Surf. Sci. Nanotech. Vol. 9 (2011) 40-45 Conference - NSS-6 -

Application of a Modulating Technique to Detect Near-Field Signals Using a Conventional IR Spectrometer with a Ceramic Light Source*

Michio Ishikawa,† Makoto Katsura, and Satoru Nakashima
Department of Earth and Space Science, Graduate School of Science, Osaka University, 1-1 Machikaneyama, Toyonaka, Osaka 560-0043, Japan

Kento Aizawa and Tsutomu Inoue
JASCO, 2967-5 Ishikawa, Hachioji, Tokyo 192-8537, Japan

Yuka Ikemoto
JASRI/SPring-8, 1-1-1 Kouto, Sayo, Hyogo 679-5198, Japan

Hidekazu Okamura
Department of Physics, Graduate School of Science, Kobe University, 1-1 Rokkodai, Nada, Kobe, Hyogo 657-8501, Japan

(Received 18 October 2010; Accepted 6 January 2011; Published 11 February 2011)

The goal of the present study is to obtain broadband near-field infrared (IR) spectra by combining Fourier-transform infrared spectroscopy (FTIR) with scattering near-field optical microscopy (s-SNOM). A stage was added to the IR spectrometer with a ceramic light source in order to modulate the probe-sample distance, and the second harmonic component was extracted by a lock-in amplifier. The detected IR signal intensity decreased exponentially with the distance between the probe tip and an Au mirror, with a localization scale of approximately 100 nm. An area with Au islands formed by electron beam lithography was scanned with the modulation system with mapping steps of X = 80 nm and Y = 133 nm. The obtained IR intensity image matches the topographic image, indicating sub-micron spatial resolution. These results indicate that the addition of the modulation system to the broadband near-field IR spectrometer was successful in obtaining localized near-field signals and sub-micron spatial resolution, even using a ceramic IR light source. [DOI: 10.1380/ejssnt.2011.40]

Keywords: Atomic force microscopy; Lithography; Infrared absorption spectroscopy; Nano-scale imaging, measurement, and manipulation technology

I. INTRODUCTION

Near-field optics has been increasingly employed in material sciences for the fabrication of nano-structures and their characterization [1, 2]. Aperture-type fiber probes and metal cantilever tips have generally been used for near-field visible and Raman spectroscopies. On the other hand, infrared (IR) spectroscopy is more versatile in disciplines such as biological, material, and earth sciences [3], even for living cells and organic compounds, which can be damaged by laser sources. However, available infrared transmitting fiber probes have low transmittance and high cost. Enhancement of near-field light signals around a metal tip is reported to be only 10- to 1000-fold in the mid-infrared region, whereas the enhancement in the visible region is millions of times [2]. Moreover, unlike visible near-field spectroscopy, the same wavelength of IR light as the incident light source is detected. Therefore, the detection of IR near-field signals was difficult.

In order to overcome these difficulties, IR near-field optics has been developed by various research groups.

In conjunction with JASCO Co., we connected a near-field optics with a scattering probe tip to an IR spectrometer with a ceramic light source to obtain wide band spectra (approximately 1000 to 5000 cm^{-1}) [4]. However, the obtained IR signals included scattered lights other than that from the probe tip, *the background scattering* [5].

Keilmann *et al.* used an IR laser source to increase IR intensity and a probe modulation system to reduce *the background scattering*. They obtained near-field IR images having a spatial resolution of less than 30 nm [6]. However, the spectral bandwidth is limited to approximately 300 cm^{-1}(approximately 800 to 1100 cm^{-1}) due to the laser source [7].

In the present study, a modulation system was added to the above-described scattering probe with the broadband IR source to reduce *the background scattering*.

II. EXPERIMENTAL

A. FT-IR + Near-Field Probe

We first describe the former near-field system without a modulation detection. A Fourier transform IR spectrometer (FTIR) was combined with near-field (NF) optics (Fig. 1). The ceramic IR light source from the FTIR is focused by a Cassegrainian mirror onto an apertureless probe tip placed within several tens of nanometers from the sample surface. This probe tip scatters near-field signals that are localized around the probe-sample region.

*This paper was presented at the 6th International Workshop on Nano-scale Spectroscopy and Nanotechnology (NSS-6), Kobe University Centennial Hall, Kobe, Japan, 25-29 October, 2010.

†Corresponding author: mishikawa@ess.sci.osaka-u.ac.jp

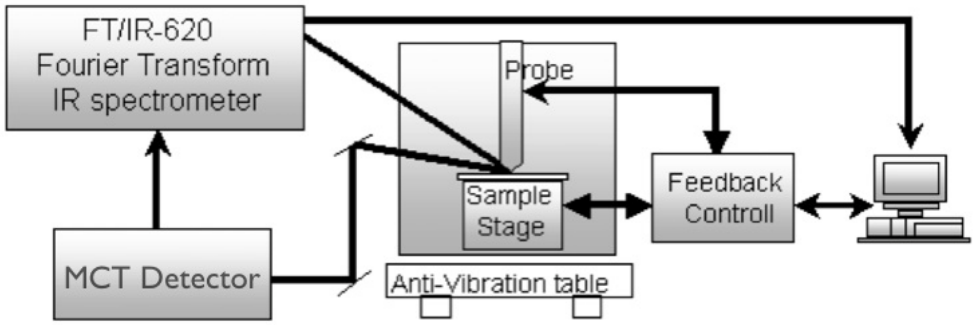

FIG. 1: Schematic system configuration of the previous near-field infrared (NF-IR) microspectrometer.

Another Cassegrainian mirror, oriented in the 90° direction from the incident Cassegrainian direction, collects this scattered light.

The scattering-type near-field probe was made of a quartz optical fiber etched by a buffered hydrogen fluoride solution [8] and then coated with gold film by sputtering. The radius of the probe tip was approximately 300 nm, which is the primary determinant of the spatial resolution of the system. The probe tip is oscillated at its resonant frequency of approximately 13 kHz. The sample is mounted on a piezoelectric XYZ stage. When the sample surface is approached to within a few tens of nanometers from the probe tip, the oscillation amplitude is decreased as a result of 'shear force' interaction with the sample [9]. A laser is illuminated on the probe tip, and the power of the reflected laser light is detected by a Si photo detector. The modulation of this signal provides a measure of the amplitude of the probe's oscillation.

This signal is then applied to a feedback system, which controls the height (Z) position of the piezoelectric stage in order to maintain a constant separation between the probe tip and the sample surface. By recording the Z value as the sample is raster scanned in the XY plane, a topographic map of the sample surface may be constructed.

B. Modulation System

In the present study, the incident IR beam is vertically polarized by placing an Au wire grid polarizer in the FTIR optics and is applied by a Cassegrainian mirror to the horizontal sample surface with a beam angle of approximately 45° (Fig. 2).

A piezoelectric actuator is placed beneath the probe tip on the sample stage to modulate the probe-sample distance. The actuator is oscillated with an amplitude of approximately 300 nm peak-to-peak by applying an AC voltage of approximately 15 V peak-to-peak at a frequency (Ω) of 2 or 3 kHz. Scattered IR signals are collected by another Cassegrainian mirror at 90° from the incident direction and are detected by an MCT detector. The second harmonic component (2Ω) is extracted by a lock-in amplifier (PerkinElmer instruments Model 5105) [10] (Fig. 2).

The intensities of the second harmonic component of scattered IR signals were detected without moving the Michelson interferometer, and these intensities can be referred to as the integral intensity. By moving the interferometer, the IR signal ranged from 1000 to 5000 cm^{-1}.

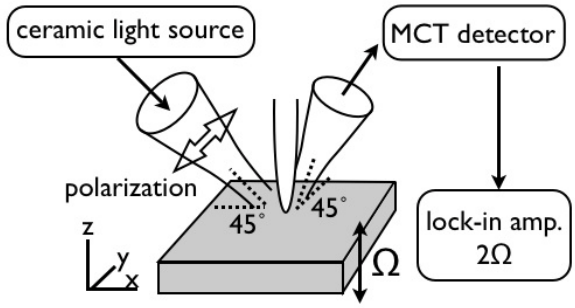

FIG. 2: A piezoelectric actuator placed beneath the probe tip is oscillated with a frequency of Ω, and the second harmonic component 2Ω is extracted by a lock-in amplifier through the MCT detector.

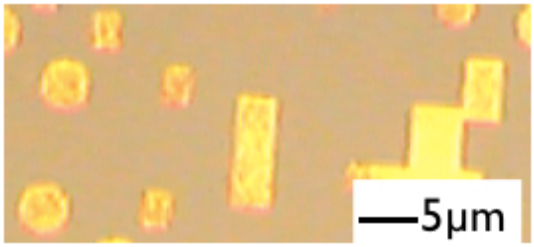

FIG. 3: Laser scanning confocal microscopic image of a standard sample fabricated by electron beam lithography. Micrometer-sized Au islands (brighter area) are distributed on a Si surface.

C. Sample Preparation

A standard sample was fabricated by electron beam lithography. An organic film (ZEP-520A, ZEON Co.) was coated on a Si plate, and an electron beam was applied to draw various patterns. The electron-damaged organic portions were dissolved by a solvent (pentyl acetate) and were coated with Au to a thickness of approximately 100 nm. The organic film was then removed by another solvent (NN dimethylacetamide solution). Micrometer-sized Au islands or border straight lines of Au were finally obtained on the Si surface (Fig. 3).

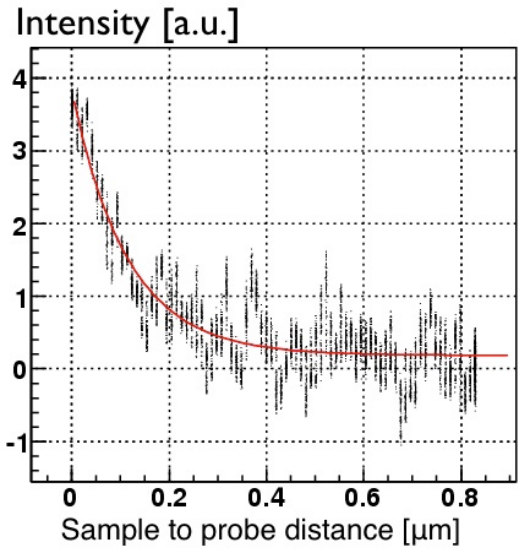

FIG. 4: Integral intensities as a function of the distance between the probe tip and an Au mirror. IR signals decreased drastically within 200 nm.

III. RESULTS AND DISCUSSION

A. Signal Localization

The distribution of IR integral intensities around the probe tip was measured while the feedback system was turned off by increasing the distance by 10 nm steps between the probe tip and an Au mirror placed on the piezoelectric actuator (Fig. 2). Here, the 0 nm position is taken as the shortest distance of probe oscillation stability. The integral intensities decrease exponentially with the distance (Fig. 4).

This decrease could be well fitted by Eq. (1) with the fitting parameters $A = 0.187 \pm 0.006$, $B = 3.63 \pm 0.02$, and $C = 0.114 \pm 0.001$ μm.

$$A + Be^{-x/C} \tag{1}$$

Parameter B (approximately 3.6) is the maximum amplitude of the near-field component. The noise level increases with the sample distance but its origin is unknown. If we fix the sample distance at 50 nm, then the noise level (approximately 0.5) is approximately 17% of the total signal intensity (approximately 3) (Fig. 4). Parameter A (approximately 0.2) may correspond to the residual scattered light not from the probe tip, despite the extraction of second-harmonic components. This residual signal is only approximately 5% of the maximum IR intensity.

Parameter C (approximately 100 nm) is the localization scale of the near-field signals. This localization scale is of the same order as the radius of the probe tip (approximately 300 nm) used in this measurement. The exponential decay of IR signals with a localization scale of approximately 100 nm indicates that near-field IR signals can be successfully extracted by this modulation system, even using a ceramic IR light source.

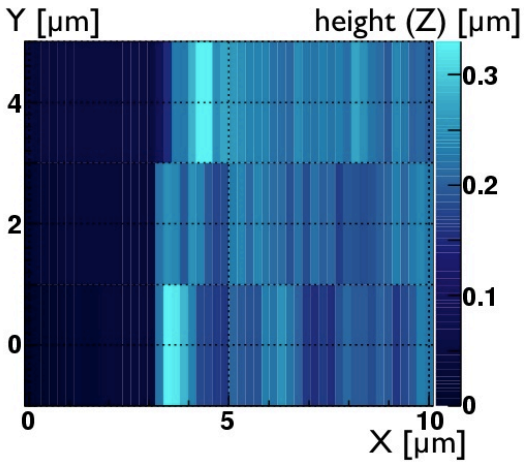

FIG. 5: Two-dimensional topographic image showing the border line between Si (0 μm< X < 3 μm) and Au (3 μm< X < 10 μm) fabricated by electron beam lithography (Fig. 3).

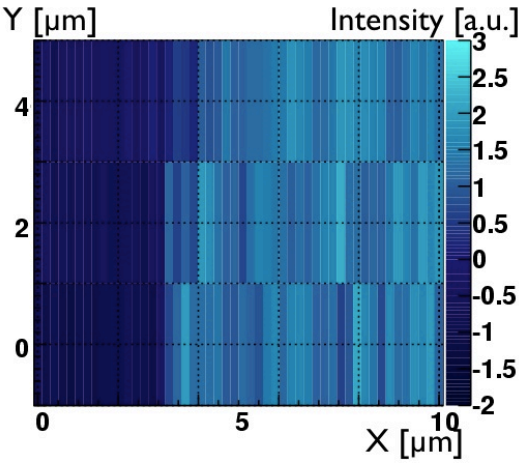

FIG. 6: IR integral intensity image of the Si (0 μm< X < 3 μm) /Au (3 μm< X < 10 μm) border after phase correction.

B. Near-Field Signal Mapping on the Si/Au Border

Using the present modulation system, the integral intensity image and topographic image can be obtained at the same time by XY mapping measurement. Figure 5 shows a topographic image of the Si/Au border, which was corrected for hysteresis (see APPENDIX A) (measurement time: approximately 400 s, measurement area 10×4 μm^2 : X = 200 nm $\times$ 50 steps, Y = 1,333 nm $\times$ 3 steps).

Figure 6 shows an integral IR intensity image of the same range.

Since the lock-in phase shift was observed at different locations, it was adjusted so as to maximize integral IR intensity on the Au position (see APPENDIX B).

The 2nd row of Fig. 6 was extracted to obtain a line profile of the IR intensity across the Si/Au border (Fig. 7). The line profile shows a rapid jump of IR intensity of within hundreds of nanometers, which is of the same order as the radius of probe tip (approximately 300 nm).

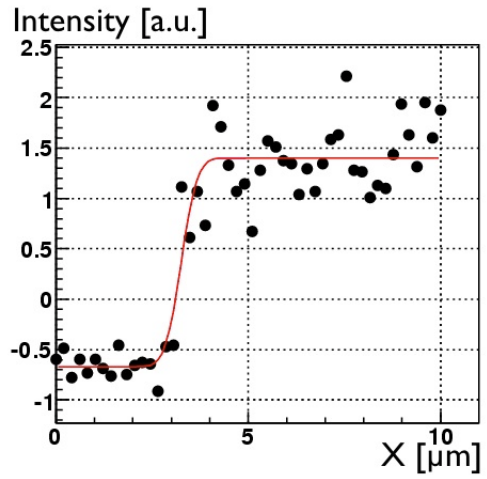

FIG. 7: IR intensity profile of the 2nd row of Fig. 6. The border line of Si and Au is at X = 3 μm.

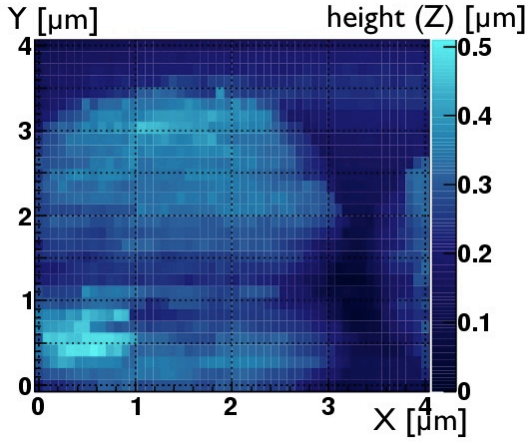

FIG. 8: Topographic image of an area with Au islands. The brighter areas are Au coated on Si. The small bright area (X, Y = 0.5 μm, 0.5 μm) may be a dust particle attached to the surface of the sample.

C. Near-Field IR Signal Mapping on Au Islands

Finally, an area with Au islands on the Si surface fabricated by electron beam lithography (Fig. 3) was mapped for integral IR intensities, together with the topographic image (Fig. 8). A total of 50 × 30 points were measured for the 4 × 4 μm^2 area, resulting in stepping sizes of X = 80 nm and Y = 133 nm (measurement time: 30 min).

The topographic image indicates the presence of an Au island area of approximately 3 μm together with an edge of another Au island to the right (Fig. 8). The IR integral intensity image obtained in this area (Fig. 9) generally agrees with the Au islands. Since the IR intensity image (Fig. 9) reveals the separation between two Au islands of approximately 500 nm, which is the same order of separation as the topographic image (Fig. 8), sub-micron spatial resolution was achieved by the present integral IR intensity measurement.

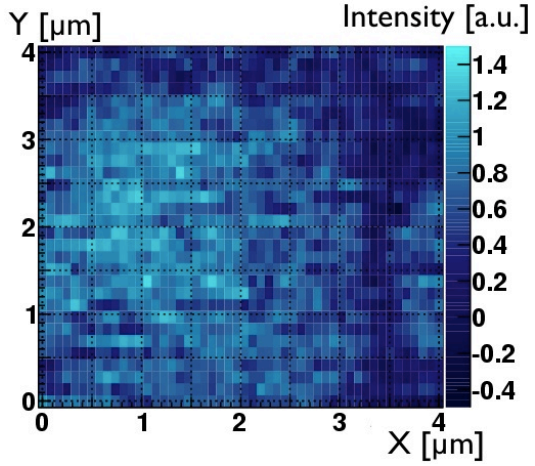

FIG. 9: IR integral intensity image of the same area shown in Fig. 8. The brighter areas of IR integral intensity matched the areas coated with Au.

IV. CONCLUSION

In order to overcome difficulties in obtaining broadband near-field IR signals with a ceramic IR source, a modulation system was added to the IR spectrometer. The Au-coated SiO_2 probe tip (radius: 300 nm) was oscillated at approximately 13 kHz. The integral IR signals in primarily the 1000 to 5000 cm^{-1} range scattered by the probe tip were detected by an MCT detector. A piezoelectric actuator was placed on the XYZ sample stage and was oscillated at an amplitude of 300 nm with a frequency (Ω) of approximately 2 or 3 kHz. The second harmonic component (2Ω) was extracted by a lock-in amplifier. The following results were obtained by this modulation measurement:

1. The detected IR signal intensity decreased exponentially with the distance between the probe tip and an Au mirror, with a localization scale of approximately 100 nm.

2. An Si/Au border was measured. The integral IR intensity image after phase correction agrees with the topographic image. The resolution is less than 1 μm.

3. An area with Au islands formed by electron beam lithography was scanned with mapping steps of X = 80 nm and Y = 133 nm. The obtained IR intensity image matches the topographic image, indicating sub-micron spatial resolution.

All of these results indicate that the addition of the modulation system to the broadband near-field IR spectrometer was successful in obtaining localized near-field signals at sub-micron spatial resolution, even using a ceramic IR light source.

Further improvements are necessary in order to establish broadband near-field IR spectroscopy. Near-field IR integral intensity signals primarily in the range from 1000 to 5000 cm^{-1} have been detected without moving the Michelson interferometer. Various wavelength-dependent methods with high signal-to-noise ratios should be tested in order to obtain near-field IR spectra and sub-micron scale maps of selected IR bands.

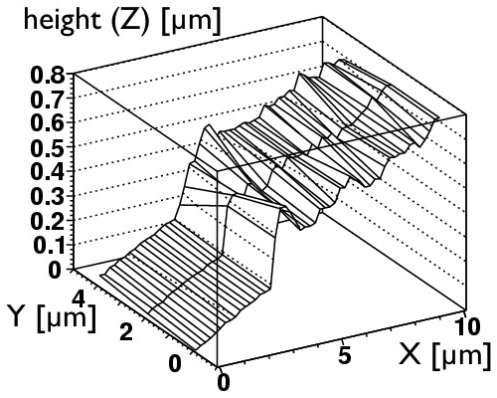

FIG. 10: Raw data of a topographic image of a border line between Si (0 μm< X < 3 μm) and Au (3 μm< X < 10 μm) fabricated by electron beam lithography (Fig. 3).

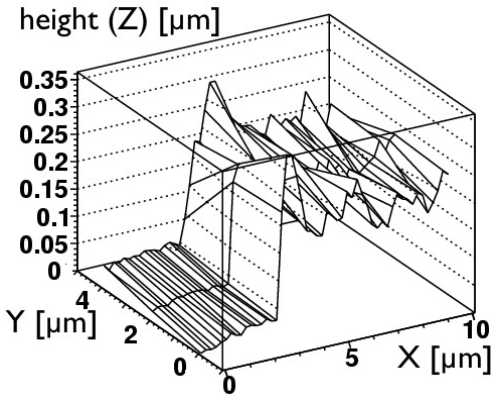

FIG. 11: Corrected topographic image of Fig. 10 showing the border line between Si (0 μm< X < 3 μm) and Au (3 μm< X < 10 μm).

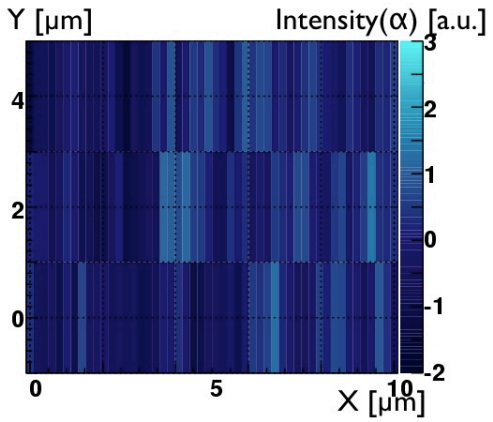

FIG. 12: In-phase component (α) image of detected IR signals on the Si (0 μm< X < 3 μm) / Au (3 μm< X < 10 μm) border.

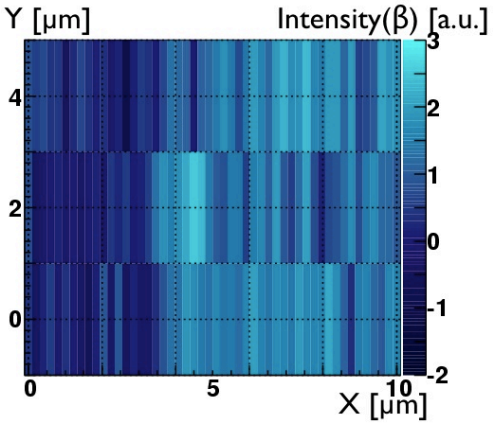

FIG. 13: Out-of-phase component (β) image of detected IR signals on the Si (0 μm< X < 3 μm) / Au (3 μm< X < 10 μm) border.

Acknowledgments

Fabrication of standard samples by electron beam lithography was supported by Professor Hirokazu Tada, Dr. Masato Ara, and the Osaka University Trans-disciplinary Graduate and Refresher Programs for Education, Research, and Training in the Fields of Nanoscience and Nanotechnology (OU-NANOPROGRAM).

M. I. was supported by a Research Assistantship form the Graduate School of Science, Osaka University and a JASRI Research Studentship.

Appendix A: Hysteresis Correction for Topographic Images

Using the present modulation system, IR integral intensity images and topographic images can be obtained simultaneously by XY mapping measurement. Unfortunately, the topographic images are always inclined (Fig. 10). The inclination is not always linear but is sometimes parabolic and originates from not only sample tilting but also the hysteresis of the piezoelectric stage. Therefore, this hysteresis was corrected by subtracting appropriate planes (Fig. 11). For example, a topographic image of a border line of Si and Au with 200-nm and 2000-nm steps in the X and Y directions (Fig. 10) can be corrected for hysteresis in order to obtain the corrected topographic image (Fig. 11).

Appendix B: Phase Corrections for Near-Field IR Signals

Integral IR intensities from the MCT detector were divided by the lock-in amplifier into an in-phase component (α) (Fig. 12) and an out-of-phase component (β) (Fig. 13) while measuring the Si and Au border lines. The Si/Au borders do not match the in-phase IR signals but rather the out-of-phase IR signals. The piezoelectric XYZ stage might have partially followed the vibration of Z-modulation piezoelectric stage, and the IR signal phase might have shifted. The phase change can also occur as a result of the differences in optical properties of Au and Si [7, 11]. However, the origin of the phase shift remains unclear.

In order to analyze the phase shift, a correlation diagram of in-phase (α) and out-of-phase (β) components was constructed (Fig. 14). The XY positions of data points reflect the radial distances (r) and the angles (θ) in the polar coordinate system. The angles (θ) correspond to phase delays with respect to the reference signal at the

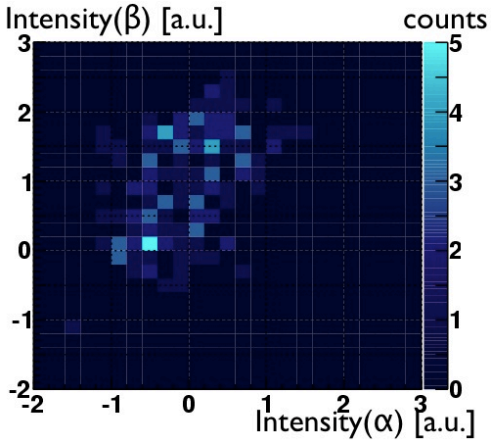

FIG. 14: Correlation of the in-phase component (α) and the out-of-phase component (β) . The two peaks at approximately (-0.5, 0) and (0, 1.5) correspond to Si and Au positions, respectively.

lock-in amplifier.

The correlation diagram shows primarily two peaks around (-0.5, 0) and (0, 1.5). By comparing the α and β values with Figs. 12 and 13, these peaks are found to correspond to Si and Au positions, respectively. The phase reference position of the lock-in amplifier was adjusted so as to maximize the integral IR intensity at the Au position in order to correct the observed phase shift.

[1] M. Ohtsu (Ed.), *Near-Field Nano/Atom Optics and Technology* (Springer-Verlag, Tokyo, 1998).
[2] S. Kawata (Ed.), *Near-Field Optics and Surface Plasmon Polaritons* (Springer-Verlag, Berlin, 2001).
[3] J. M. Hollas, *Modern Spectroscopy*, 3rd ed. (John Wiley and Sons, Chichester, 1996).
[4] N. Kuya, S. Nakashima, S. Okumura, M. Nakauchi, S. Kimura and Y. Narita in *Physicochemistry of Water in Geological and Biological Systems*, Eds. S. Nakashima, C. J. Spiers, L. Mercury, P. A. Fenter, and M. F. Hochella, Jr. (Universal Academy Press, Inc., Tokyo, 2004), p. 179.
[5] Y. Kebukawa, S. Nakashima, M. Ishikawa, K. Aizawa, T. Inoue, K. Nakamura-Messenger, and M. E. Zolensky, Meteoritics and Planetary Science **45**, 394 (2010).
[6] B. Knoll and F. Keilmann, Nature **399**, 134 (1999).
[7] S. Amarie, T. Ganz, and F. Keilmann, Optics Express **17**, 21794 (2009).
[8] S. Mononobe and M. Ohtsu, J. Lightwave Technol. **14**, 2231 (1996).
[9] E. Betzig and J. K. Tarautman, Science **257**, 189 (1992)
[10] B. Knoll and F. Keilmann, Optics Communications **182**, 321 (2000).
[11] R. Hillenbrand and F. Keilmann, Phys. Rev. Lett. **85**, 3029 (2000).